Simulation and measurement of relief effects on passive microwave radiation

LI Xinxin[1,2], **ZHANG Lixin**[1,2], **JIANG Lingmei**[1,2], **ZHAO Shaojie**[1,2], **ZHAO Tianjie**[1,2]

1. *State Key Laboratory of Remote Sensing Science, Jointly Sponsored by the Institute of Remote Sensing Applications of Chinese Academy of Sciences and Beijing Normal University, Beijing* 100875, *China*;
2. *School of Geography and Remote Sensing Science, Beijing Normal University, Beijing* 100875, *China*

Abstract: Based on the theory of the relief effects on passive microwave radiation, we think that it is necessary to do the experiments in the field by observing the different topographic landscapes we design and compare the data we observe with the simulations of relief effects modeled by AIEM. The result shows there are 10-15 K bias of brightness temperatures affected by the tilted angles between flat terrain and mountainous terrain. When the frequencies are less than 10 GHZ, the relief effects of terrain elevation becomes weakening. Therefore, we certified that microwave polarization paths and directions have obviously changed due to the surface geometrical property, such as shape and the orientation of hills.

Key words: relief effects, passive microwave radiation, experiment, AIEM

CLC number: TP701/TP721.1 **Document code:** A

Citation format: Li X X, Zhang L X, Jiang L M, Zhao S J and Zhao T J. 2011. Simulation and measurement of relief effects on passive microwave radiation. *Journal of Remote Sensing*, **15**(1): 100–110

1 INTRODUCTION

The signal of a microwave radiometer observing a land surface from space is composed of surface and atmospheric contributions, both of which depend on the relief (Matzler *et al.*, 2000). Hillslope-scale topography influences microwave brightness temperatures in a way that produces bias at coarser scales. In a previous study using digital elevation models (DEM), it is found that the modeled brightness temperatures in areas of variable topography can be several kelvins different more than a corresponding flat surface (Kerr, *et al.*, 2003). Talone, *et al.* (2007) used a 30 m DEM and a 100m land cover map to derive inputs to the SMOS RTM, in which the DEM is used to incorporate topographic effects on shadowing and local incidence angles. Furthermore, Mialon, *et al.*, (2008) discussed relief effects in the context of the SMOS mission and developed a criterion to identify SMOS 4 K accuracy. The works of Sandells, *et al.*, and Matzler, *et al.*, (2000) are notable because they include the effects of topographic slope on the geometry of observation. Recently, Alejandro *et al.*, (2009) demonstrated the effect of topographic variability, and topography significantly affects the spatial distribution of modeled brightness temperature. Guo (2009) developed topographic correction of microwave radiation model based on AMSR-E, only existing about 2 K brightness temperature bias. In these studies, relief effects are considered quite significant for microwave radiation on land, but are devoid of experiment validating.

Accordingly, the objectives of this paper are twofold: (1) Field-data-supported selection and verification of an appropriate physically based surface emission model; (2) the generation of comprehensive relief factors in microwave radiation transmission. A description of the physical theory underlying modeling microwave radiation emission on terrain follows in Section 2. Section 3 demonstrates that topographic effects simulation. Then we present an overview of the field experiments conducted to clarify the effects of terrain in Section 3. We present the comparison between the model simulation and field-data in Section 4. Finally, Conclusions arise from our experiments and simulations.

2 MODELING MICROWAVE RADIATION ON TOPOGRAPHY

Relief effects on microwave radiation are composed of four factors, which are topographic elevation, slope angle, aspect, and terrain shadow. As the factors of relief effects, they have their corresponding influence on the path through the atmosphere, the observed angle, the polarized orientation and a total brightness temperature of observed footprint, respectively. Any one of the relief effect factors would alter the brightness

Received: 2010-03-12; **Accepted**: 2010-07-17

Foundation: The National Basic Research Program of China (973 Program) (No. 2007CB714403); The European Union FP7 Program——Qinghai-Tibet Plateau Soil Moisture Inversion Program (No.212921).

First author biography: LI Xinxin (1985—), female, Ph. D. candidate. She majors in passive microwave remote sensing of soil moisture and the relief effects on multi-frequency microwave. E-mail: lixx213@mail.bnu.edu.cn

temperature observed by a microwave radiometer or the effective emission. To investigate the potential of passive microwave for observing topography, it is essential to build the relief landscape based on the vehicular microwave radiometer observation. This paper reports on the study supported by the field data and seeks to improve our understanding of relief effects on the microwave radiation at microwave frequencies.

Brightness temperatures obtained from the field experiment are converted to apparent (effective) emissivity by using the simple relationship.

$$Tb=eTs \tag{1}$$

where e is the emissivity, Ts is the physical temperature of the surface, Tb is brightness temperature. When we consider relief effects, microwave radiation transmission on topography can be described as:

$$Tb_{\text{top}} = F(\theta_{\text{l}},\varphi,S_{\text{R,Sun}},h,Tb_{\text{,hills}})\times e_{\text{flat}}\times Ts_{\text{flat}} \tag{2}$$

where Tb_{top} is brightness temperature on topography, e_{flat} is land emission on flat, Ts_{flat} is land physical temperature on flat, $F(\theta_{\text{l}}$, φ, $S_{\text{R,Sun}}$, h, $Tb_{\text{,hills}})$ is the function of relief factors, contained local incident angles θ_{l}, polarization rotation angles φ, shadow factors $S_{\text{R,Sun}}$, elevation h, and co-hill brightness temperature $Tb_{\text{,hills}}$.

3 SIMULATION ANALYSES

Before the relief experiment, it is important to simulate the impact of topographic factors on microwave radiation features. Among the physically based models, the advanced integral equation model (AIEM) has a much wider application range of surface roughness conditions than that of conventional models (Shi, *et al.*, 2002). Used AIEM describing surface emission, relief factors are input to the relief emission calculation, which model relief effects on microwave radiation. Among relief factors surface elevation can be ignored when the observed frequencies are less than 10 GHz, so that our study selects C band (6.925 GHz) and X band (10.25 GHz). Except elevation, for a sloping surface, local incident angles that the observing satellite makes with the reference location is a function of the local topographic slope and aspect. Here hill slopes and aspects are input to AIEM by using the flowing relationships (Matzler, *et al.*, 2000):

$$\cos\theta_{\text{l}} = \cos\alpha\cos\theta + \sin\alpha\sin\theta\cos(\phi-\beta) \tag{3}$$

where θ_{l} is the local incident angle transformed from the global to the local plane of incidence, α is the tilt angle, θ is the observation angle with respect to the surface normal, ϕ is the azimuth angle of the observed view, β is the aspect of tilted surface.

Simultaneously, the aspects of tilted surface will alter polarized direction according the earth reference frame, called "polarization rotation". Furthermore the linear polarization is rotated by an angle φ, given by

$$\sin\varphi = \sin(\phi-\beta)\sin\alpha/\sin\theta_{\text{l}} \tag{4}$$

The emissivity $E_{\text{V}}(\theta)$ and $E_{\text{H}}(\theta)$ in rolling terrain can be represented:

$$\begin{aligned} E_{\text{V}}(\theta) &= E_{\text{V}}(\theta_{\text{l}})\cos^2\varphi + E_{\text{H}}(\theta_{\text{l}})\sin^2\varphi \\ E_{\text{H}}(\theta) &= E_{\text{V}}(\theta_{\text{l}})\sin^2\varphi - E_{\text{H}}(\theta_{\text{l}})\cos^2\varphi \end{aligned} \tag{5}$$

Parameters in the relief effects model need to input, such as the soil volumetric moisture is about 25%, surface correlation length is 100 cm and root mean square height is 0.5 cm, observed angle is 55°, and the observed frequency is 6.925 GHz.

Tilted surface unconcerned with polarization rotation manifests the microwave radiation character related on hill slopes. Fig.1(a) describes the relationship between surface emission and local incident angles affected by hill slopes only. It can be seen that there are some obvious differences between horizontal polarization and vertical polarization while slopes are less than 40°. This result plays a basic role on the experiment so that all relief landscape we built over 40°. When it is concerned with polarization rotation, the microwave radiation of tilted surface becomes more complex. Fig.1(b) shows the change of the surface emission with the polarization rotation angles. It is a symmetry curve at ϕ=0° for both polarizations. Thus it can be seen that the polarization rotation is formed under positive-negative angles, so the terrain shape generates multi-aspect angles in the relief landscape is more important than the rotation.

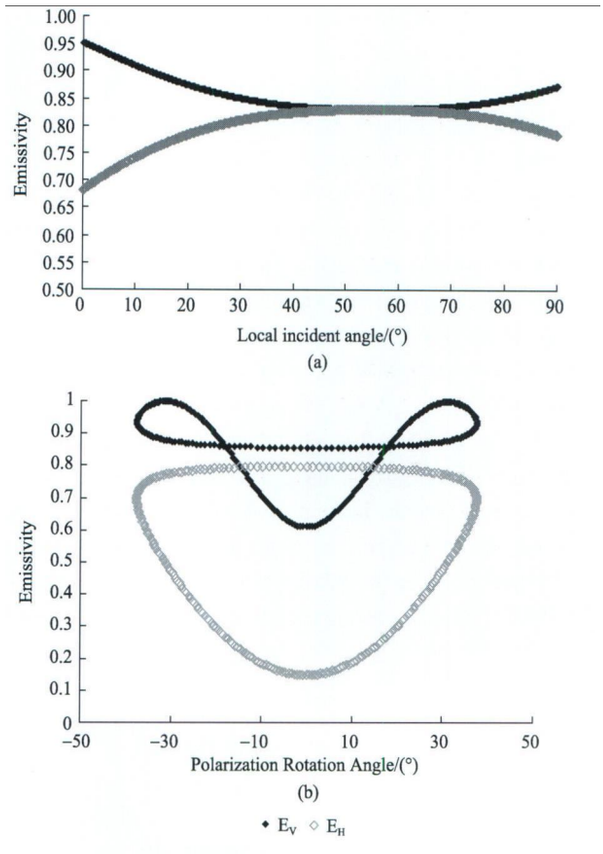

Fig. 1 Simulation of local incident angle impact on surface emission at 6.925 GHz frequency by AIEM
(a) without polarization rotation; (b) with polarization rotation

Shadow effects are depicted as shadow area weighted brightness temperature sums (Matzler, *et al.*, 2000). Terrain

shadow refers to two kinds, one is the shadow of the sun direction, and the other is invisible area due to radiometer observing. These shadows and non-shaded area constitute together the whole view of observing footprint which can be represented shaded facets and non-shaded ones. It will be our follow-up study in the future.

4 EXPERIMENT

To research relief effects more in-depth on surface emission at the microwave frequency, we design a controlled field experiment. The field site is in the Field Test Site of Baoding in Hebei province. The target footprint is 4 m × 4 m and is set out miniature hills such that they are simulated landform landscape. We level the surface as best as we can put up hills first. Then we pile two kinds of hills in different surface configuration using shovels and the wooden batten. To regulate the moisture content of hills, we carried local soil from the same source. To observe brightness temperatures, we use a truck-mounted microwave radiation (TMMR). The TMMR configuration comprised a six-channel that covers the frequency ranges of 6.925 GHz, 10.65 GHz, 18.7 GHz, 23.8 GHz, 36.5 GHz, and 89 GHz at both vertical and horizontal polarizations. Soil moisture measurement is done by can samples. From the can sample, we additionally obtain the bulk density of the soil. Soil surface temperature is measured by the infrared temperature sensor. Fig. 2 shows the relief observation setup.

To argue relief effects on microwave radiation, we designed a controlled field experiment based on twofold: (1) the size of miniature hills; (2) the shape of miniature hills. All of hills are not higher than 2 m and also far less than the height of TMMR, so that can be prone to the observation. Keeping hills visible completely, we also regulate the observed area of hills by their height. Considering diversification of hill slopes, prismy hills are piled by fluvo-aquic soil, and their shape insure the observed surface area in a certain direction of view without polarization rotation. Prismy hills is built in different slopes (0°, 10°, 20°, 30°). When dealing with the variational aspects at each observed facet, we put up conical hills so that it can obtain surface emission under the impact of polarization rotation. Fig. 3 shows the several hills we build at different slope angles. Table 1 shows the various settings and conditions of targets. Fig. 4 exhibits a series of relief landscape views we project.

Fig. 2 Setup of the field experiment

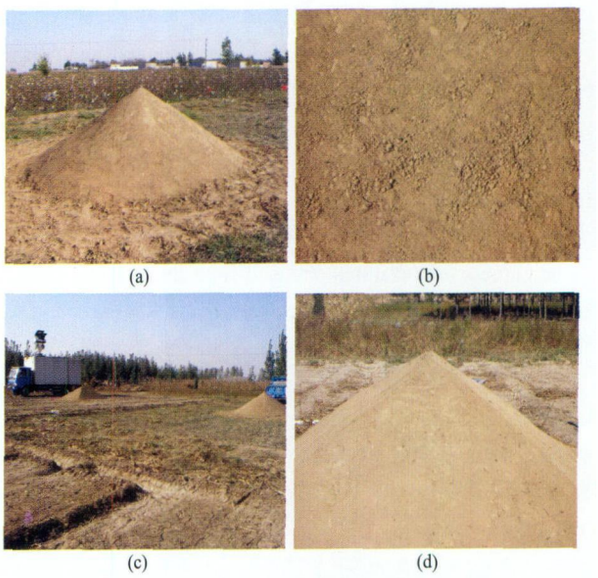

Fig. 3 Four views of relief landscape

(a) The conoid hill; (b) Surface of hills; (c) Prismy hill and conoid hill observed by the truck-mounted microwave radiometer; (d) observed prismy hill

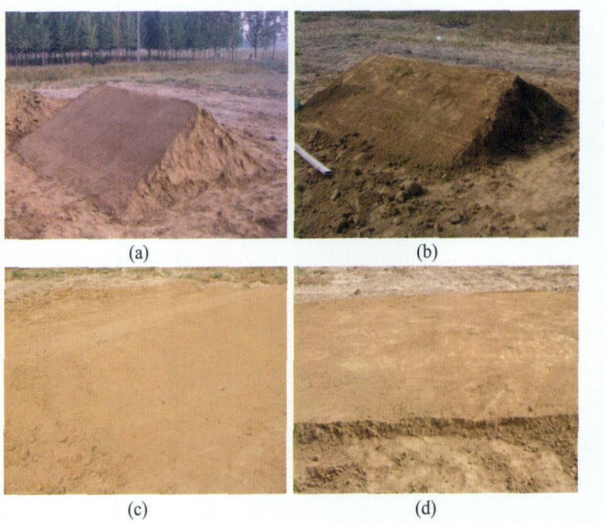

Fig. 4 Views of relief landscape of different slopes: 30°, 21°, 10°, and 0° prismy hills

(a) 30°; (b) 21°; (c) 10°; (d) 0°

Table 1 Experiment Conditions

Observable quantity	Soil type	Soil moisture	Soil temperature	Soil sandy content	Soil clay content
Value	fluvo-aquic soil	12.8% v/v	15.8℃	51.7% v/v	8.2% v/v

In summary, the observation steps are given as follows.

Step 1 Set up flat field on footprint

Step 2 Observe flat field

Step 3 Take soil samples

Step 4 Set up prismy hills in different slopes, but in accordant size

Step 5 Observe prismy hills

(1) Observe brightness temperature

(2) Take temperature measurement

(3) Take soil sample

Step 6 Observe conical hills

(1) Observe brightness temperature

(2) Take temperature measurement

(3) Take soil sample

Step 7 Repeat step 5 and step 6 for different desired slope conditions.

Step 8 Collect soil and close down (TMMR)

5 RESULTS AND DISCUSSION

Brightness temperatures obtained from the field experiment were converted to effective emissivity by using Eq.(1) in Section 2. The Dobson model (Dobson, *et al.*, 1985) is the dielectric models used in theoretical calculations of the dielectric constant.

To achieve simplicity the following conventions are followed in representing the employed microwave radiation features: (1) the surface emissivity obtained from the experiment are abbreviated as E_V_obs and E_H_obs; (2) the effective emissivity computed by relief simulation based on AIEM are predigested as E_{VAIEM} and E_{HAIEM}; (3) H or V indicates the polarization of the channel with H being horizontally polarized and V being vertically polarized.

Fig.5 shows a comparison of observation and simulation data for prismy hills and flat field at 6.925 GHz. The observation of the overall trend between emissivity and local incident angle is consistent with the simulation. The simulated model generally underestimates the values for both polarizations. V polarization has a better agreement than H polarization. For H polarization, we note an apparent disagreement between the data sets at lower slopes (or higher local incident angles). The degree of discrepancy increases with increasing local incident angles. We conclude that it is not suitable for the applications at lower slope terrain in the present simulation based on AIEM. At the mean time, we know the discrepancy between V and H polarization where the slope is less than 40° is mainly resulted by much lower slopes of tiled surface (<20°). However, we find that when we rectified surface roughness condition the disagreement between the simulation and the observation is obsolete. Fig. 6 shows the comparison between simulation and observation after inputting roughness parameters (rms height is 1 cm, correlation length is 10 cm). The triangles represent adjusted results at lower slopes.

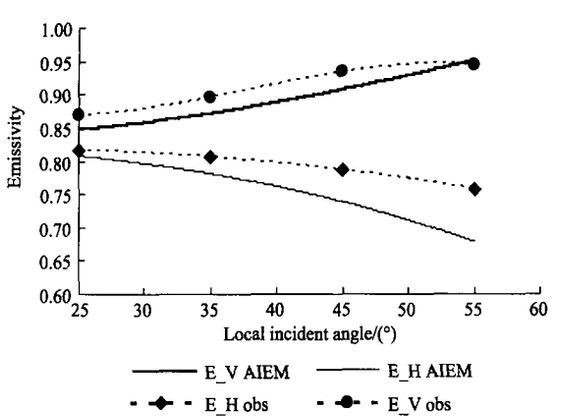

Fig. 5 Results of observed data compared with simulation at C band

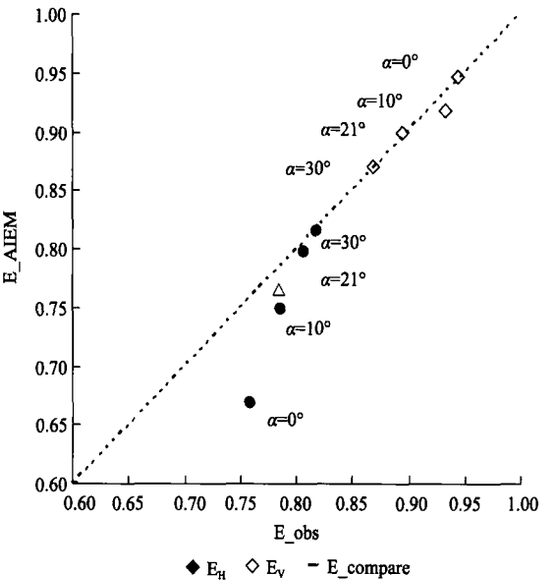

Fig. 6 Comparison of observed data and simulation after roughness regulation at C band

Surface topography also results in a rotation of the linear polarization by a polarization rotation angle. Polarimetric ratios are more indicative of geometric or shape properties of the target, rather than dielectric or local illumination conditions. Ratios are calculated using temperature units for radiometry (Woodhouse, 2006). The ratio of vertical to horizontal signal, r is given by

$$r = \frac{T_V}{T_H} \tag{6}$$

T_V and T_H were obtained from observing prismy hills and conic hills. Fig. 7 demonstrates that for conic hill, polarimetric ratio R(H, V) varies obviously according to polarization rotation angles. But for prismy hill conversely, there is smaller degree of change in R(H, V). Because microwave radiation of observed facets transformed under their multi orientation with aspects of conic hills from 0° to 360°, by contrast, prismy hills only with one orientation observed. It can be seen polarization rotation is affected by shape property; many kinds of terrain shape have various polarization; the aspect change can cause polarization rotation, therefore, shape is also one of the relief factors.

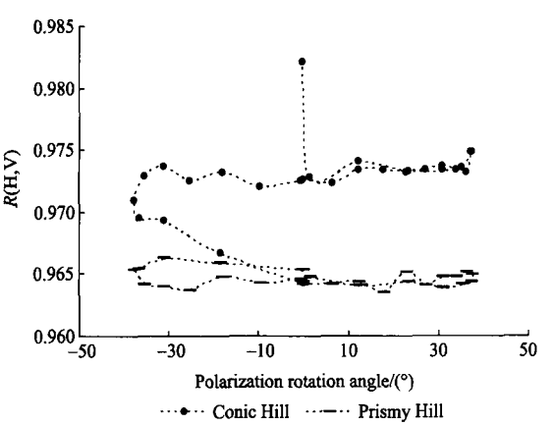

Fig. 7 Polarization rotation with polarimetric ratio in different shape hills

While observing at band X (>10GHz), Fig. 8 shows the lower accuracy of the comparison between the field data and the simulation than that at band C. Affected by atmosphere, it should be considered elevated surface affects emission at band X. We also deem that the atmosphere effects for elevation can be eliminated at band C.

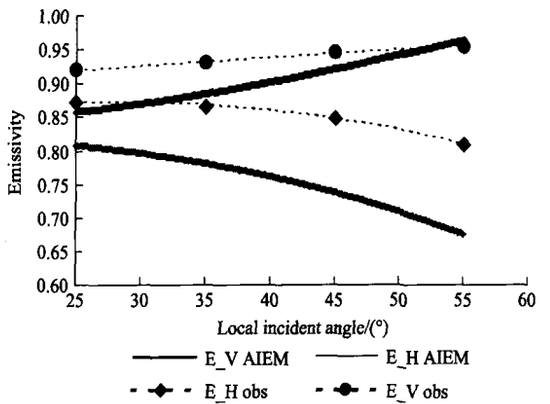

Fig. 8 Results of observed data compared with simulation at band X

6 CONCLUSIONS

Topographic effects on microwave radiation play a significant role in modeling hill slope-scale brightness temperatures. Local incident angle and polarization rotation associated with topography both are relief variation in modeled hillslope-scale brightness temperatures. Previous studies have reported that the topographic contrasts in the surface states that control emission of microwave radiation based on modeling. In this study the topographic modeling combined with field experiment in order to discuss relief effects on the basis of measurement.

Results grounded on field experiments indicate hillslope and higher slope angles result in both small-scale variability in surface states and a wide range of local incident angles. Spatial heterogeneity in the surface states affects the spatial distribution of hillslope-scale brightness temperatures. Our field experiment and model validation confirms that AIEM can be used to simulate surface emission reasonably well under roughness conditions in mountainous area. The simulation is significantly improved if the effects of rough surface are incorporated into the model in the case of small angles.

The geometric property of land surface affects microwave polarizations which is denoted by polarized ratio R(H, V). By comparing distinct shape property of piled hills, we found that topographic shape can transfer microwave polarization, coming into polarization rotation angles. Therefore, the shape property in topography is one of the relief factors, like local incident angles.

At 6.925 GHz, a transparent atmosphere for topography makes elevation ignored in relief effects by comparing with the observation at 10.25 GHz. We demonstrate that not all of microwave frequencies can be the atmospheric window.

According to our study, there is about 10—15 K brightness temperature bias, for v polarization the relief effects become smaller and smaller with the augment of slopes; for h polarization, inversely with the slope change. However, we still have problem with the error between the observation and the topographic simulation at h polarizations, which need further research.

Due to the limitations in our field experiment setup, it is recommended that more field or laboratory experiments with truly topographic be conducted to conclusively validate the significance of the relief effect. Our future experiment will consider topographic shadowing and whether atmospheric effects can be ignored at lower frequency as those considered in this paper.

REFERENCES

Alejandro N Flores, Valeriy Y Ivanov, Dara Entekhabi and Rafael L Bras. 2009. Impact of hillslope-scale organization of topography, soil moisture, soil temperature, and vegetation on modeling surface microwave radiation emission. *IEEE Transactions on Geoscience and Remote Sensing*, **47**(8): 2557–2571

Dobson M C, Ulaby F T, Hallikainen M T and El-rayes M A 1985. Microwave dielectric behavior of wet soil—Part II: Dielectric mixing models. *IEEE Transactions on Geoscience and Remote Sensing*, **23**(1): 35–46

David N Kuria, Toshio Koike, Hui Lu, Hiroyuki Tsutsui and Tobias Graf. 2007. Field-supported verification and improvement of a passive microwave surface emission model for rough, bare, and wet soil surface by incorporating shadowing effects. *IEEE Trans. Geosci Remote Sens*, **45**(5): 1207–1216

Guo Y. 2009. Study on terrain correction of passive and active microwave measurements and soil moisture retrieval combining passive and active microwave remote sensing. Biejing: Chinese Academy of Sciences

Kerr Y, Secherre F, Lastent J and Wigneron J P. 2003. SMOS: Analysis of perturbing effect cover land surfaces. *Proc. IGARSS*, **2**: 908–910

Matzler C. and Standley A. 2000. Technical note: relief effects for passive microwave remote sensing. *International Journal of Remoth Sensing*, **21**(12): 2403–2412

Mialon A, Coret L, Kerr Y H, Secherre F and Wigneron J P. 2008. Flagging the topographic impact on the SMOS signal. *IEEE Trans. Geosci. Remote Sens*, **46**(3): 689–694

Sandells M J, Davenport I J and Gurney R J. 2008. Passive L-band microwave soil moisture retrieval error arising from topography in otherwise uniform scenes. *Adv. Water Resour*, **31**(11): 1433–1443

Shi J C, Jiang L M and Zhang L X. 2006. A parameterized multi-frequency-polarization surface emission model. *Joumal of Remote Sensing*, **10**(4): 502–514

Talone M, Camps A, Monerris A, Vall-llossera M, Ferrazzoli P and Piles M. 2007. Surface topography and mixed-pixel effects on the simulated L-band brightness temperatures. *IEEE Trans. Geosci. Remote Sens*, **45**(7): 1996–2003

Woodhouse M. 2006. Introduction of Microwave Remote Sensing. American: Science Press: 65–82

被动微波辐射特征地形效应模拟与实验

李欣欣[1,2], 张立新[1,2], 蒋玲梅[1,2], 赵少杰[1,2], 赵天杰[1,2]

1. 遥感科学国家重点实验室 北京师范大学, 北京 100875;
2. 北京师范大学 地理学与遥感科学学院, 北京 100875

摘 要: 基于地形对被动微波辐射的影响机理研究, 利用 AIEM 模型模拟微波辐射的地形效应, 建立实验地貌微缩景观, 由车载微波辐射计进行观测, 探索影响被动微波辐射特征的地形因子。地基实验表明, 在低频波段本地入射角对山地倾斜表面的微波辐射有 10 K—15 K 的影响, 小于 10GHz 的观测频率可以消除地形高度对微波辐射的影响。同时, 实验验证微波极化受地表形态属性——山体坡向和山体形状的影响显著, 地形坡度对极化信息影响不明显。

关键词: 地形效应, 被动微波辐射, 地形实验, AIEM

中图分类号: TP701/TP721.1 **文献标志码:** A

引用格式: 李欣欣, 张立新, 蒋玲梅, 赵少杰, 赵天杰. 2011. 被动微波辐射特征地形效应模拟与实验. 遥感学报, 15(1): 100–110
Li X X, Zhang L X, Jiang L M, Zhao S J and Zhao T J. 2011. Simulation and measurement of relief effects on passive microwave radiation. *Journal of Remote Sensing*, 15(1): 100–110

1 引 言

地形是地物和地貌的总称, 包括地势与天然地物和人工地物的位置在内的地表形态。微波辐射计观测地表的信号来自于空间范围内地表和大气的整体贡献, 不论是地表还是大气辐射能量都会受到地形的影响。影响地表微波辐射特征的地形主要是指像元尺度上的山地地形, 区别于地形在波长尺度的地表粗糙度影响。特别是在山区, 由于地形造成微波辐射亮度温度观测偏差, 影响微波遥感地表参数反演精度。

探讨微波辐射地形影响的各项研究都表明, 山坡尺度的地形(约几十米)对大尺度(几十公里)微波辐射计观测亮温可能产生几十至几百开尔文的辐射能量偏差。如 Kerr 等(2003)将数字高程模型(DEM)融入模型研究中, 发现在有地形起伏变化的地区模拟得到的亮温值与平坦地表模拟值相比有十几开尔文的偏差。Talone 等(2007)用 30 m 分辨率的 DEM 和 100 m 分辨率的地表覆盖图作为 SMOS 辐射传输模型的输入参量, 其中地形影响采用由 DEM 得到的阴影和本地入射角表达。更进一步, Mialon 等(2008)讨论了阴影和本地入射角在 SMOS 计划中的影响, 并发展了一项准则用以识别 SMOS 观测的像元亮温在地形的影响下观测误差是否满足不大于 4 K 的要求, 但由于采用 L 波段卫星微波辐射观测, 空间分辨率进一步降低, 即便是全球大范围连续地形起伏区域对该波长范围的观测影响也表现得很小, 在反演土壤水分等地表参数时, 其反演误差在允许精度范围(<4%)。Sandells 等(2008)及 Matzler 和 Standley (2000) 的研究所做的贡献尤为显著, 他们从观测几何视角出发考虑, 由视场内的多种几何角度表达了地形坡度的定量化影响。近期, Alejandro 等(2009)将裸露地表的地形影响扩展到考虑地表多覆盖要素, 如土壤水分, 植被生物量等与地形的相关关系, 综合分析了多地表因素影响下的辐射计观测亮温的空间分异性。中国已有研究者郭英(2009), 在被动微波辐射研究中基于 AIEM 模型的模拟, 定量分析和评价了本地入射角、极化旋转和阴影对地表发射率的影响, 在此基础上提出了基于被动微波像元尺度的地形校正算法, 该算法验证表明只有 2 K 左右的地形亮温偏差, 缺乏真实地表地形实验的验证。

本研究基于被动微波辐射地形效应的理论研究, 提出可能影响微波辐射特征的地形因子, 通过开展地基微波辐射观测实验, 建立微缩地貌场景, 研究

收稿日期: 2010-03-12; **修订日期:** 2010-07-17
基金项目: 国家重点基础研究发展计划(973 计划)(编号: 2007CB714403)和欧盟 FP7 计划 "青藏高原土壤水分产品反演" (编号: 212921)。
第一作者简介: 李欣欣(1985—), 女, 陕西人, 博士研究生, 从事微波遥感领域研究。E-mail: lixx213@mail.bnu.edu.cn。

本地入射角等地形因子对裸露地表发射率的影响，并与改进的积分方程模型(AIEM)模拟地形效应进行对比分析，结果表明不同地形因子对地形的不同变化产生了相应影响，使地形观测亮温较之平坦地表有十几开尔文的偏差。

2 山区裸露地表微波辐射传输

山地指由山岭和山谷组合而成的高地。沿一定构造线延伸的岭谷相间的山体称为山脉。通常将有成因联系并按一定延伸方向的一组山脉，称为山系。地形在微波辐射中的作用(地形效应)主要会表现在以下几方面:

(1) 大气光学厚度将会随着海拔高度的变化而改变，使得地表辐射能量因地形引起传输路径的改变;

(2) 地表起伏变化致使微波发射表面倾斜，辐射计观测角转换为本地入射角，由于倾斜表面的多方向性发生极化旋转，地表发射率因角度变化而改变;

(3) 地形的邻近效应。受山体间的相互辐射影响，部分观测场景会被遮蔽，观测场景地表辐射中可能包含其他山地的入射能量，如果地表形态的变化与波长同阶，则会发生衍射。

(4) 地形阴影效应。山体的起伏形态对平坦地表以及部分山体形成遮蔽，被遮挡的像元自身发射的微波辐射信号也随之被减弱，降低了观测地表对辐射计接收信息的贡献率。

(5) 山体太阳辐射源方向性影响，形成阴阳坡面。阴坡上的像元接受到较弱的照度而具有较低的亮度值，阳坡上的像元接受到较强的照度而具有较高的亮度值，致使处在阴坡和阳坡的同类地物的象元亮度值相差较大。

辐射计观测地形景观亮温值 Tb 通过下式转换为地表发射率 e(David, 2007):

$$Tb=eTs \tag{1}$$

式中，Ts 为地表土壤物理温度。

山体的坡度坡向信息，山体海拔高度，山体间电磁波辐射等都是影响山区微波辐射传输的地形因子。在低频波段(<117GHz),可以对 Plank 公式近似，得到Rayleigh-Jeans公式的近似，由此可得微波辐射亮温的简化表达式，考虑地形影响，山区微波辐射传输方程可以表达为:

$$Tb_{\text{top}} = F(\theta_{\text{l}}, \varphi, S_{\text{R,Sun}}, h, Tb_{\text{hills}}) \times e_{\text{flat}} \times Ts_{\text{flat}} \tag{2}$$

式中，Tb_{top} 是地形影响下的微波辐射亮温，e_{flat} 表示平坦地表发射率，Ts_{flat} 是平坦地表物理温度，$F(\theta_{\text{l}}, \varphi, S_{\text{R,Sun}}, h, Tb_{\text{hills}})$表示地形效应函数，函数自变量是地形因子分别为本地入射角、极化旋转角、辐射计与太阳共同形成的地形观测阴影、海拔高度、连续山体间的相互辐射。

3 地形效应模拟

地形效应模拟其目的在于为地基辐射计观测实验提供先验知识，有助于设计实验方案和控制实验条件，并在实验后与观测数据进行对比分析，进而探索影响微波辐射的地形因子。改进的积分方程(AIEM)针对被动微波辐射计观测，适用于模拟宽波段和大角度的地表辐射信号(施建成，等 2006)，本研究应用 AIEM 计算平坦裸地发射率。地形因子——本地入射角的计算，采用 Matzler 等(2000)提出的计算公式:

$$\cos\theta_{\text{l}} = \cos\alpha\cos\theta + \sin\alpha\sin\theta\cos(\phi-\beta) \tag{3}$$

式中，本地入射角 θ_{l} 由坡度 α，坡向 β，辐射计观测角 θ，以及山体方位角 ϕ 计算得到。同时极化旋转角计算公式如下:

$$\sin\varphi = \sin(\phi-\beta)\sin\alpha/\sin\theta_{\text{l}} \tag{4}$$

式中，φ 表示极化旋转角。山体的海拔高度主要影响电磁波的大气传输路径，在微波辐射传输过程中，当频率小于 10 GHz 时，可以忽略大气的影响(Woodhouse, 2006)，因此模拟采用频率为 6.925 GHz 的 C 波段。具体模拟参数如表 1。

表 1 地形效应模拟 AIEM 输入参数

频率 GHz	观测角度 /(°)	土壤介电常数实部	土壤介电常数虚部	表面相关长度/cm	均方根高度/cm
6.925	55	5.431	0.642	10	1

以表 1 的输入为模拟参数，受地形影响的地表发射率可由下式表示:

$$\begin{aligned} E_{\text{V}}(\theta) &= E_{\text{V}}(\theta_{\text{l}})\cos^2\varphi + E_{\text{H}}(\theta_{\text{l}})\sin^2\varphi \\ E_{\text{H}}(\theta) &= E_{\text{V}}(\theta_{\text{l}})\sin^2\varphi - E_{\text{H}}(\theta_{\text{l}})\cos^2\varphi \end{aligned} \tag{5}$$

式中，E_{V} 和 E_{H} 分别表示垂直极化和水平极化地表发射率。

山区倾斜表面发射率随坡度的变化如图1 所示。当坡度取值范围是 0—90°，计算山区倾斜表面 1000 个模拟点的发射率随山体坡度的变化，当坡度不大于 40°时水平极化与垂直极化差异特征明显，易于对比分析，易于堆建地形景观的实现。当考虑山体的形状和方向等几何特征时，电场极化坐标系发生旋转，极化旋转角作为地形因子同样会影响微波辐射特征，如图 2 所示。图 2 曲线变化显示了山体几何特征会使地表微波辐射变得更加复杂，呈现出在极

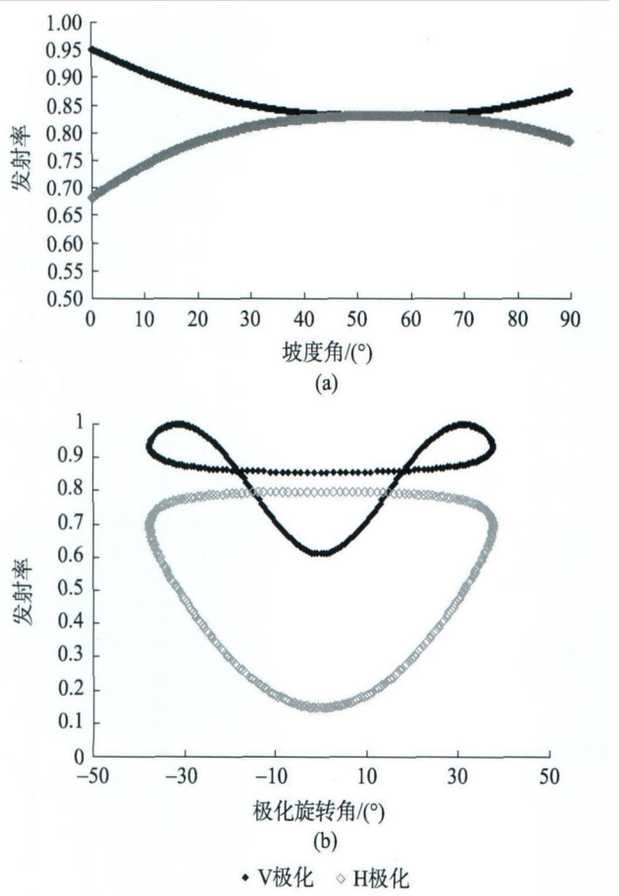

图 1 本地入射角与极化旋转角模拟结果

(a) 山区倾斜表面地形效应模拟; (b) 坡度为 30°, 坡向在 2π空间内变化的倾斜表面地形效应模拟

化旋转角 φ=0°处的对称变化。H 极化发射率在极化旋转角取得极值处达到最大值，在 φ=0°两侧发射率随着 φ 的绝对值的增大而增大。V 极化发射率在 φ=0°两侧随着 φ 绝对值的增大在 φ=30°和−30°时取得最大值，当 φ 的绝对值大于 30°时，随着角度的增加地表发射率呈下降趋势，并在 φ 取极值处达到稳定，不再发生变化。H 极化方式和 V 极化方式其发射率的最小值均是在 φ=0°时取得。

基于以上模拟分析，为了更清晰地描述地形效应在两种极化方式下分别对微波辐射的影响，实验中控制山体坡度不大于 40°，且鉴于极化旋转的复杂性需要在实验中设计山体的几何形态，并结合适当的观测频率选择，更进一步考察地形所受的大气影响。

4 实 验

基于以上地形效应初探，开展地基微波辐射计观测实验。

4.1 实验概况

实验于 2009-10-19 在河北省保定市清苑县冉庄的一片开阔空旷的裸土区域进行，实验主要观测设备是车载微波辐射计测量地表辐射亮度温度，并配有热红外测温仪探测土壤温度，坡度仪测量地形坡度，以及烘箱等测量土壤水分。将测量的土壤质地数据输入 Dobson 模型计算土壤介电常数(Dobson 等，1985)。非成像车载微波辐射计设有 6 个观测频率，分别是 6.925, 10.65, 18.7, 23.8, 36.5, 以及 89 GHz，水平和垂直两种极化方式，具体的辐射计性能参数如表 2 所示。图 2 展示了实验场的建立概况。

表 2 微波辐射计系统主要技术指标

项目	性能指标
系统噪声温度/K	<500
辐射分辨率/K	0.5
接收机和天线热稳定性/K	<0.05
天线旁瓣水平/dB	< −30
辐射测量范围/K	0—350
工作环境温度/℃	−30—45
天线观察方位角范围/(°)	0—360
天线观察俯仰角范围/(°)	−90—90
天线最大上升高度/m	8.20
系统峰值功率/kW	< 3
供电系统功率/kW	5

图 2 车载微波辐射计观测地形实验场

4.2 实验方法与过程

实验采取局部变量控制法建立地形微缩场景。控制观测环境条件(大气、土壤的湿度温度等)，通过设计不同形态的山体，控制山体的形状、坡度、表面粗糙度，同时使山体的土壤质地和土壤水分含量保持一致。图 3 表示车载辐射计半功率波束宽度的视场范围，其中红线代表 C 波段，蓝线代表 X 波段，距主波瓣的垂直距离最近，则信号强度也最强，所以实验中选择了最近辐射计观测视场，以最小圆的直径，−3 dB 为 3 m 长，−10 dB 直径长 4 m，以此做为地形场的底边长。据此构建了满足不同地形因子独

立观测的地形景观，图 4 展示了地形实验的主要观测场景。有关地形场景参数如表 3。

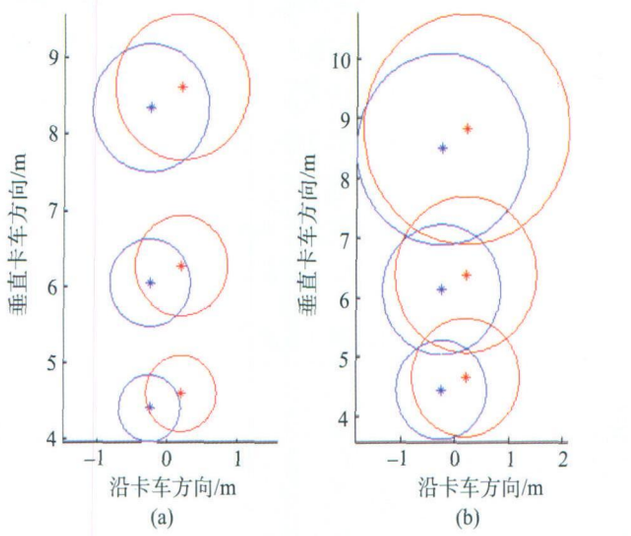

图 3 辐射计视场范围

(a) –3 dB 波束宽度的视场范围; (b) –10 dB 波束宽度的视场范围

图 4 辐射计观测地形场景

(a) 圆锥状山体; (b) 山体的表面状况; (c) 辐射计的观测状况; (d) 棱柱形山体

表 3 地形景观土壤参数

土壤类型	土壤体积含水量 /cm³/cm³	土壤温度 /℃	土壤砂粒含量/%	土壤粘粒含量/%
黄砂质潮土	0.128	15.8	51.7	8.2

实验观测采用两种观测频率，小于 10 GHz 的 C 波段，和大于 10 GHz 的 X 波段。在不考虑山体高度的条件下，C 波段观测不同坡度的倾斜表面本地入射角对微波辐射特征的影响，为了保证辐射计只观测到固定方位的斜面，实验设计了棱柱状山体(图 5)，并且与 X 波段观测相比较验证地表高度对观测频率的响应。堆建圆锥状山体考察地形对微波极化特征的影响，圆锥上每个面元的坡向变化范围是 0°—360°，使电磁波的极化发生旋转。具体的实验步骤如图 6 流程图所示。实验中可能存在的观测误差来自于两方面，一是天空背景的辐射，经地表反射会进入辐射计的观测信号，在观测角 55°时，经实验测量 C 波段天空辐射为 5.5 K—7.25 K, X 波段为 8.575 K—10.70 K，由倾斜地表反射，进入辐射计的天空辐射在 C 波段约为 1 K，在 X 波段约为 2 K，我们认为与测量地形的亮温值(>200 K)相比,在误差允许范围内；二是辐射计观测平台车身的辐射，经过实验前对辐射计的定标测量我们认为车体的辐射对观测的影响很小，在测量误差允许范围内。

图 5 不同坡度的地形景观

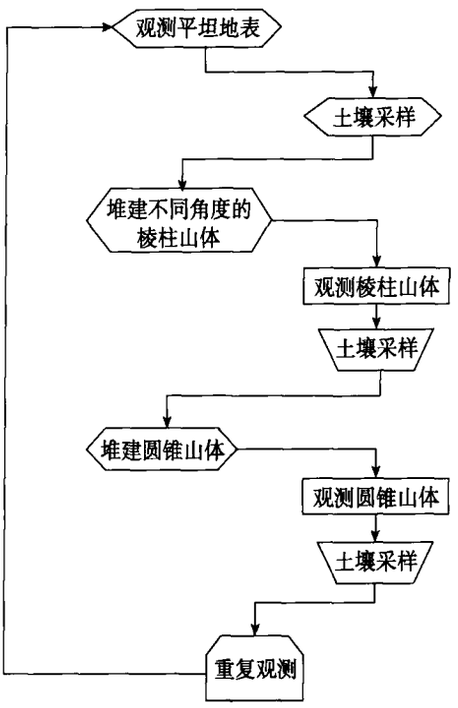

图 6 实验观测流程图

5 结果分析与讨论

实验观测结果计算显示有地形起伏地表与平坦

地表(α=0°)相比亮温值相差 10 K—15 K。为了独立考察地形的影响, 削弱表面粗糙度的影响, 在实验中将山体表面进行了平整处理, 因此, 基于 AIEM 模型的模拟中粗糙度参数也相应做出调整, 将均方根高度设为 0.1 cm, 表面相关长度设为 50 cm, 观测所得地表发射率与基于 AIEM 模型地形效应模拟的发射率值在 C 波段的对比结果如图 7 所示。对比结果显示, 地形效应模拟与实验观测表面发射率随本地入射角的变化趋势一致, 垂直极化发射率随本地入射角的增加而增加, 水平极化发射率相反, 随本地入射角的增大而降低。若假设模拟值与观测值完全相等时, 二者拟合度为 100%, 经计算垂直极化发射率拟合度为 99.68%, 水平极化拟合度为 95.25%。地形效应模拟与观测 V 极化误差变化范围是–0.3%—0.3%, H 极化误差小于 5%。H 极化误差主要是由于小角度起伏地表微波辐射特征的模拟造成的, 我们认为在微波辐射计观测中微起伏地表既要考虑本地入射角影响也受地表粗糙度的影响, 据此修改模型模拟的低起伏度地表发射率的粗糙度输入参数(均方根高度为 1 cm, 表面相关长度为 10 cm)。经过修正 H 极化拟合度为 98.01%, 平均误差小于 2%。两种极化方式在不同坡度下观测与模拟的比较, 如图 8 所示, 三角形标记为修正后对比结果。对于垂直极化在 0°—30°坡度变化范围内, 观测与模拟接近于直线“AIEM 模拟发射率”=“观测发射率”, 而水平极化只有当坡度接近 20°时模拟值与观测值才趋于一致, 实验观测在近平坦起伏地表处发射率与模拟值相差 3.5%, 这说明了基于 AIEM 模拟的地形效应在微波水平极化传输中与实验观测的倾斜表面的辐射特征存在差异, 而垂直极化采用 AIEM 模型与实验观测比较相差 0.17%, 能更好的模拟地表微波辐射特征。

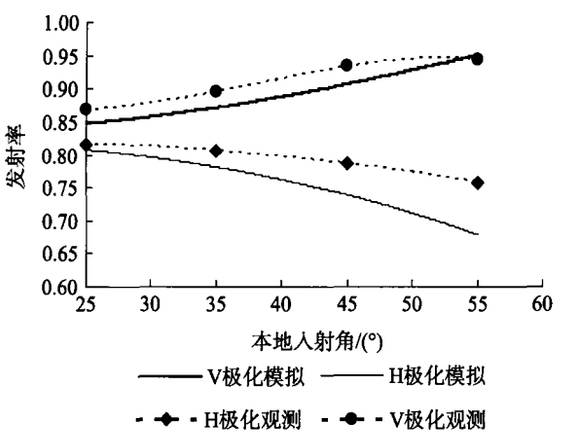

图 7 C 波段微波辐射特征地表发射率的观测值与模拟值对比(AIEM)

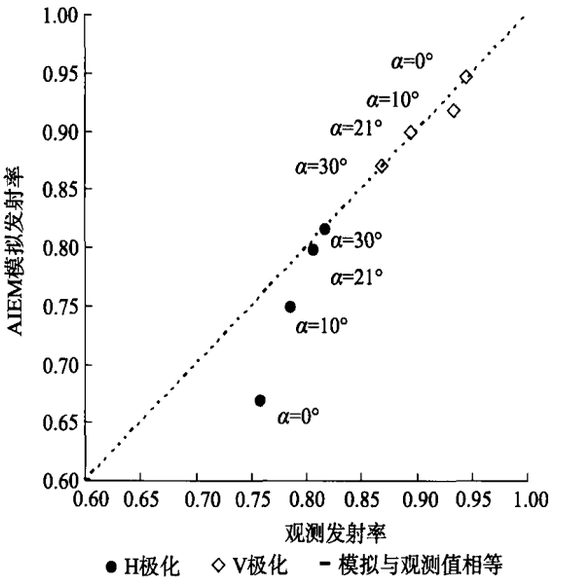

图 8 V 极化与 H 极化不同坡度 α 的表面发射率比较

为了考察极化旋转发生条件, 分别对固定方位单斜面棱柱山体(Prismy Hill)和 360°方位变化的圆锥山体(Conic Hill)进行观测, 极化旋转变量由水平极化与垂直极化的亮度温度之比——微波辐射极化指数 R(H,V)来表示, R(H,V)指示 H 和 V 极化在电磁波传播方向上的方向变化性(Woodhouse, 2006), 若 R(H, V)用 r 表示, 则 r 的计算公式如式(6)所示。

$$r=\frac{T_V}{T_H} \tag{6}$$

式中, T_V 和 T_H 分别表示垂直极化和水平极化的亮度温度观测值。

如图 9 所示, 观测结果发现圆锥山体的微波极化指数 R(H,V)随着极化旋转角的变化发生明显的方向性旋转, 其 R 指数最大变化达到 2%, 棱柱山体较之前者极化没有发生明显旋转变化, 仅有 0.01%的变化。这说明了极化主要受地表形态参数(形状和方向)的影响, 当观测面元的方位角发生变化则极化旋转发生。

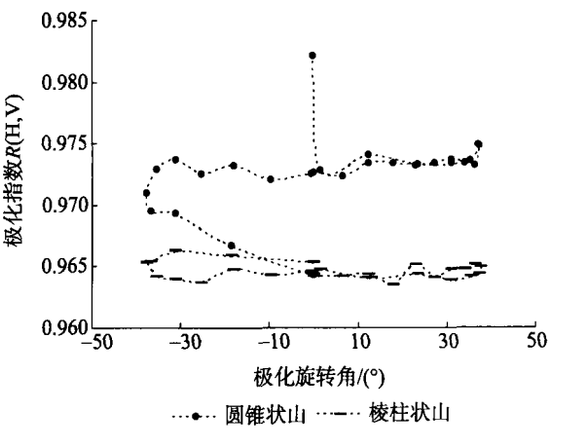

图 9 不同形状山体的微波辐射极化变化

同时，实验中也采用 X 波段对地形场景进行观测，目的是考察地形因子表面高度对微波辐射的影响。仍采用 C 波段的基于 AIEM 模拟与观测对比的方法，保持与 C 波段观测条件一致，其结果如图 10。V 极化模拟与观测误差达±4%，H 极化误差为±8%，拟合精度比 C 波段明显下降，说明选择低频波段观测可以降低表面高度对微波辐射的影响，大于 10 GHz 的观测频率需要考虑海拔高度这一地形因子的作用。

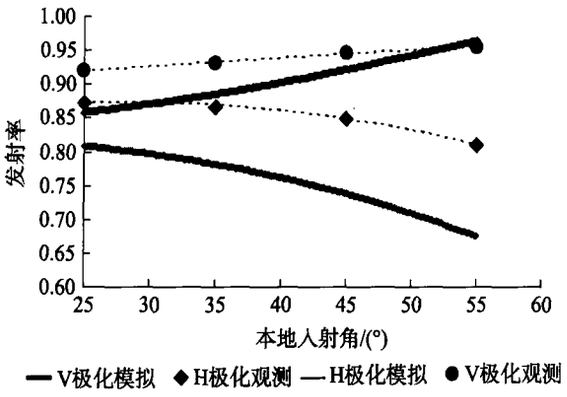

图 10 X 波段微波辐射特征地表发射率的观测值与模拟值对比(AIEM)

6 结 论

实验观测微缩地形景观，结合基于 AIEM 的地形效应模拟，研究被动微波辐射特征地形效应。研究表明，倾斜地表坡度引起辐射计观测角度发生变化，在低频波段(6.925 GHz)，地形模拟与观测结果拟合精度达到 94%—99%，本地入射角对山区微波辐射影响明显，可以采用 AIEM 模型模拟山区倾斜表面地形影响，实验验证满足误差精度要求(<4%)。影响微波极化的地形因子——山体的形状和坡向使极化坐标系发生旋转，由简单微波极化指数 R(H, V)响应极化旋转角的变化。地形海拔高度又与大气传输过程相联系，利用微波低频消除海拔高度的地形影响是本研究中对比两个最靠近临界频率(10 GHz)的波段——C 和 X 波段的意义之所在。但 H 极化与 V 极化可由模型解释的成分有差异，V 极化能较好地由 AIEM 地形模拟解释，而 H 极化在有 2%的误差需要进一步研究，得到更准确的解释。未来将考虑对影响微波辐射的地形阴影进行实验研究。

REFERENCES

Alejandro N Flores, Valeriy Y Ivanov, Dara Entekhabi and Rafael L Bras. 2009. Impact of hillslope-scale organization of topography, soil moisture, soil temperature, and vegetation on modeling surface microwave radiation emission. *IEEE Transactions on Geoscience and Remote Sensing*, **47**(8): 2557–2571

Dobson M C, Ulaby F T, Hallikainen M T and El-rayes M A 1985. Microwave dielectric behavior of wet soil—Part II: Dielectric mixing models. *IEEE Transactions on Geoscience and Remote Sensing*, **23**(1): 35–46

David N Kuria, Toshio Koike, Hui Lu, Hiroyuki Tsutsui and Tobias Graf. 2007. Field-supported verification and improvement of a passive microwave surface emission model for rough, bare, and wet soil surface by incorporating shadowing effects. *IEEE Trans. Geosci Remote Sens*, **45**(5): 1207–1216

Guo Y. 2009. Study on terrain correction of passive and active microwave measurements and soil moisture retrieval combining passive and active microwave remote sensing. Biejing: Chinese Academy of Sciences

Kerr Y, Secherre F, Lastent J and Wigneron J P. 2003. SMOS: Analysis of perturbing effect cover land surfaces. *Proc. IGARSS*, **2**: 908–910

Matzler C. and Standley A. 2000. Technical note: relief effects for passive microwave remote sensing. *International Journal of Remoth Sensing*, **21**(12): 2403–2412

Mialon A, Coret L, Kerr Y H, Secherre F and Wigneron J P. 2008. Flagging the topographic impact on the SMOS signal. *IEEE Trans. Geosci. Remote Sens*, **46**(3): 689–694

Sandells M J, Davenport I J and Gurney R J. 2008. Passive L-band microwave soil moisture retrieval error arising from topography in otherwise uniform scenes. *Adv. Water Resour*, **31**(11): 1433–1443

Shi J C, Jiang L M and Zhang L X. 2006. A parameterized multi-frequency-polarization surface emission model. *Joumal of Remote Sensing*, **10**(4): 502–514

Talone M, Camps A, Monerris A, Vall-Ilossera M, Ferrazzoli P and Piles M. 2007. Surface topography and mixed-pixel effects on the simulated L-band brightness temperatures. *IEEE Trans. Geosci. Remote Sens*, **45**(7): 1996–2003

Woodhouse M. 2006. Introduction of Microwave Remote Sensing. American: Science Press: 65–82

附中文参考文献

郭英. 2009. 主被动微波遥感的地形校正与土壤水分联合反演研究. 北京: 中国科学院遥感应用研究所: 41–58

施建成, 蒋玲梅, 张立新. 2006. 多频率多极化地表辐射参数化模型. 遥感学报, **10**(4): 502–514